Proceedings of the ASME 2017 36th International Conference on Ocean, Offshore and Arctic Engineering
OMAE2017
June 25-30, 2017, Trondheim, Norway

OMAE2017-62535

HYDRODYNAMIC COEFFICIENTS OF A FLEXIBLE PIPE WITH STAGGERED BUOYANCY ELEMENTS AND STRAKES UNDER VIV CONDITIONS

Shixiao Fu
SINTEF Ocean[1], Trondheim, Norway

Halvor Lie
SINTEF Ocean, Trondheim, Norway

Jie Wu
SINTEF Ocean, Trondheim, Norway

Rolf Baarholm
Statoil, Trondheim, Norway

ABSTRACT

A 38m long flexible pipe with staggered buoyancy modules and strakes has been tested in the ocean basin of SINTEF Ocean (former Marintek) for VIV investigation of a lazy wave riser. In this paper the inverse analysis method was presented and applied into the investigation of the hydrodynamic force coefficients along this tested flexible pipe with the measured responses as inputs. The feasibility of the inverse analysis method is firstly validated by numerical simulations. The distributions of the added mass and excitation coefficients along the flexible pipe with staggered buoyancy modules and strakes are then investigated. The identified coefficients are validated by check of the natural frequencies and responses of the model, and are finally compared against those from the forced oscillation tests.

***Key words**:* hydrodynamic coefficients, staggered buoyancy elements, strakes, inverse analysis

1. INTRODUCTION[1]

As the exploitation of offshore oil resources moves into deeper waters, risers with staggered buoyancy elements and strakes have been looked as promising applications, e.g. steel lazy wave riser. Under the action of ocean current and/or top vessel motions, vortex-induced vibration (VIV) will occur on the slender cylindrical riser, which can result in severe fatigue damage. Prediction and control of this kind of VIV on risers has become crucial for the safety design of the risers, where hydrodynamic forces are the key inputs.

Hydrodynamic forces of a rigid cylinder segment oscillating in the cross flow (CF) and/or in-line (IL) directions of its moving direction have been looked as the fundamental problem for understanding and prediction of VIV of flexile riser in current. By forced oscillation tests of a rigid cylinder towed in water, Gopalkrishnan [3] and Aronsen [4] investigated the VIV hydrodynamic forces in its purely CF or IL directions, which has been widely used today by the empirical prediction programs, e.g. Shear7[5] and VIVANA[6]. Dahl [7] conducted two dimensional forced oscillation tests of the rigid cylinder, by oscillating it in both CF and IL directions simultaneously. Soni [8] and Yin and Larsen [9] studied vortex-induced force of flexible riser with realistic cross sectional orbits by forced oscillations of a rigid cylinder, where the oscillations replicated the motion at various cross-sections on a flexible riser as measured from flexible riser model tests. Wu et al. [10] obtained the vortex-induced forces and its coefficients on a bare flexible riser in the CF direction using an inverse method. Based on finite element method and modal superposition, using the strain information measured in the scaled flexile riser model test as input, Song et al. [11] firstly got the hydrodynamic force distribution on a flexible pipe, which were then decomposed into exciting(damping) and added mass force coefficients by least square method. The results show that the hydrodynamic coefficients on a flexible riser undergoing VIV are different from those of the rigid cylinder forced oscillation test.

The foregoing researches mainly focused on the hydrodynamic forces of the fully bare pipes under VIV. However, in practical application, the risers are normally attached with staggered buoyancy modules and strakes, which will then bring more complications and differences on the hydrodynamic forces acting on the risers compared with those on the fully bare risers, which have not been clarified so far.

[1] Earlier MARINTEK, SINTEF Ocean from 1st January 2017 through a merger internally in the SINTEF Group

Recently, a 38m long flexible pipe with staggered buoyancy modules and strakes has been tested in the ocean basin of SINTEF Ocean (former MARINTEK) for VIV investigation of a lazy wave riser[1]. In this paper the inverse analysis method[2] was applied to analyze the hydrodynamic forces along this tested riser, with the measured responses as inputs. The feasibility of the inverse analysis is firstly validated by the comparison between identified coefficients from VIV responses predicted by VIVANA[6] and those used during the corresponding VIV responses calculation. Based on this inverse analysis method, the distributions of the added mass and excitation coefficients along the flexible pipe with staggered buoyancy modules and strakes are then investigated. Some of the results were finally compared with the pure CF direction forced oscillation model test of a rigid cylinder with buoyancy element in the towing tank.

2. BASIC THEORY

A submerged flexible pipe with a tensional force *T* in a uniform current is illustrated in Fig. 1. The central axis of the pipe lies in the X-axis. The direction of the flow is parallel to X-Y plane and orthogonal to the pipe.

Based on finite element method, the governing equation of spatial pipe can be expressed as,

$$[M]\{\ddot{y}\}+[C]\{\dot{y}\}+[K]\{y\}=\{F\} \qquad (1)$$

where M, C and K are global mass matrix, structural damping matrix and structural stiffness matrix(including geometry stiffness from the tensional force) of the dry pipe, respectively and the detailed description can be found in Song [2]; $y, \dot{y}, \ddot{y}$ are the displacement matrix, velocity matrix and acceleration matrix in CF direction respectively; F is the CF hydrodynamic force matrix. The damping matrix C can be obtained by Rayleigh damping model.

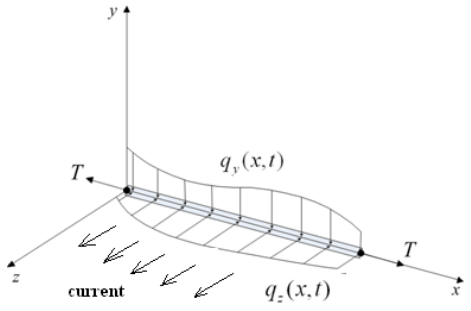

Fig. 1 Hydrodynamic forces of a submerged flexible riser with a tensional force in current

2.1 Hydrodynamic Forces

Dynamic displacements y in CF direction can be obtained by modal superposition from the measured strains [2] from VIV model testing. Meanwhile, the tensional force at each station could be acquired from the measured four strains [2] around the circumferential direction of each cross section, and were then directly used as the inputs for the calculation of the geometry stiffness of the dry structure in the subsequent analysis. In this way, the effects of the tensional forces on the stiffness of the structures were finally accounted during the inverse analysis.

The velocity $\dot{y}$ and acceleration $\ddot{y}$ can be acquired by the first- and second-order partial derivatives of displacement y with respect to time t, which could be based on central-difference scheme.

With the known left side of Eq.(1): response matrixes $y, \dot{y}, \ddot{y}$, and the structural mass, damping and stiffness matrixes, the right side of Eq. (1) F can then be directly obtained from simple mathematical operation[2].

2.2 Hydrodynamic Coefficients

Assuming that the vibration in CF direction is composed of *n* different periodical vibrations, the VIV displacement at node *z* can be expressed by summing up the contributions from each of the vibration component

$$y(x,t)=\sum_{i=1}^{n} y_{0i}(x)\sin(\omega_i t+\theta_i(x)) \qquad (2)$$

where ω_i is the i^{th} vibration frequency in CF direction, $y_{0i}(x)$ and $\theta_i(x)$ are the corresponding amplitude and phase angle at frequency ω_i .

The VIV velocity $\dot{y}(x,t)$ and acceleration $\ddot{y}(x,t)$ can then be obtained from Eq. (2):

$$\begin{aligned}\dot{y}(x,t)&=\sum_{i=1}^{n} y_{0i}(x)\omega_i\cos(\omega_i t+\theta_i(x))\\ \ddot{y}(x,t)&=-\sum_{i=1}^{n} y_{0i}(x)\omega_i^{\,2}\sin(\omega_i t+\theta_i(x))\end{aligned} \qquad (3)$$

The hydrodynamic force at node *x*, $f_{CF}(x,t)$ can be assumed to be

$$f_{CF}(x,t)=\sum_{i=1}^{n} f_{0i}(x)\sin(\omega_i t+\theta_i(x)+\varphi_i(x)) \qquad (4)$$

where $f_{0i}(x)$ is the hydrodynamic force amplitude at frequency ω_i, and $\varphi_i(x)$ is the corresponding phase angle between the hydrodynamic force and the displacement.

Expanding the right side of Eq. (4),

$$\begin{aligned}f_{CF}(x,t)=&-(-\sum_{i=1}^{n} f_{0i}(x)\sin(\omega_i t+\theta_i(x))\cos(\varphi_i(x)))\\ &+\sum_{i=1}^{n} f_{0i}(x)\cos(\omega_i t+\theta_i(x))\sin(\varphi_i(x))\end{aligned} \qquad (5)$$

where $\sum_{i=1}^{n} f_{0i}(x)\cos(\omega_i t+\theta_i(x))\sin(\varphi_i(x))$ is the hydrodynamic force in phase with the velocity $\dot{y}(x,t)$, and can be further expressed as

$$\sum_{i=1}^{n} f_{0i}(x)\cos(\omega_i t+\theta_i(x))\sin(\varphi_i(x)) = \begin{cases} \dfrac{D_{bare} l\rho U^2}{2\sqrt{2}\dot{y}_{RMS}(x)} C_{e,bare}(x)\dot{y}(x,t) & \text{for bare pipe} \\ \dfrac{D_{buo} l\rho U^2}{2\sqrt{2}\dot{y}_{RMS}(x)} C_{e,buo}(x)\dot{y}(x,t) & \text{for buoyancy module} \end{cases} \quad (6)$$

where $C_{e,bare}(x), C_{e,buoyancy}(x)$ is the excitation coefficient at node x for bare and buoyancy elements respectively, ρ is the fluid density, U is the fluid velocity, D_{bare} and D_{buo} are the diameter of the bare pipe and buoyancy elements respectively, and $\dot{y}_{RMS}(x)$ is the root mean square (RMS) value of the VIV velocity at node x. If the VIV response has only one frequency, $\sqrt{2}\dot{y}_{RMS}(x)$ is equivalent to the amplitude of the VIV velocity $\dot{y}(x,t)$.

The term $-(-\sum_{i=1}^{n} f_{0i}(x)\sin(\omega_i t+\theta_i(x))\cos(\varphi_i(x)))$ in Eq. (5) is the hydrodynamic force in phase with VIV acceleration $\ddot{y}(x,t)$; this force is referred to as the added-mass force, and can be further expressed as

$$-\sum_{i=1}^{n} f_{0i}(x)\sin(\omega_i t+\theta_i(x))\cos(\varphi_i(x)) = \begin{cases} \frac{1}{4}\rho\pi {D_{bare}}^2 l C_{a,bare}(x)\ddot{y}(x,t) & \text{for bare pipe} \\ \frac{1}{4}\rho\pi {D_{buo}}^2 l C_{a,buo}(x)\ddot{y}(x,t) & \text{for buoyancy module} \end{cases} \quad (7)$$

where $C_{a,bare}(x)$ and $C_{a,buo}(x)$ is the added-mass coefficient at node z for bare pipe and buoyancy elements respectively.

Substituting Eqs. (6) and (7) into Eq. (5) gives

$$f_{CF}(x,t) = \begin{cases} \dfrac{D_{bare} l\rho U^2}{2\sqrt{2}\dot{y}_{RMS}(x)} C_{Le,bare}(x)\dot{y}(x,t) - \frac{1}{4}\rho\pi {D_{bare}}^2 l C_{La,bare}(x)\ddot{y}(x,t) \\ \dfrac{D_{buo} l\rho U^2}{2\sqrt{2}\dot{y}_{RMS}(x)} C_{Le,buo}(x)\dot{y}(x,t) - \frac{1}{4}\rho\pi {D_{buo}}^2 l C_{La,buo}(x)\ddot{y}(x,t) \end{cases} \quad (8)$$

Given the hydrodynamic force and the VIV velocity and acceleration at node x, the excitation coefficient and added-mass coefficient can be derived by the least squares method [2].

In this paper, only the dominating one frequency was picked out for the hydrodynamic analysis, therefore, the n=1 for all the above equations.

3. EXPERIMENTAL DISCRIPTION

In year of 2015, NDP tested a 38m long flexible straight pipe with staggered buoyancy modules and strakes in Marintek ocean basin for VIV investigation on a lazy wave riser[1]. The staggered riser model was towed with uniform moving speed and the strain along the pipe were measured by fiber optical in four quarters along the circumferential direction of each measuring station: two sensors in CF direction and two in IL direction.

Figure 2 illustrates the typical arrangement and main parameters definition of the buoyancy elements configuration.

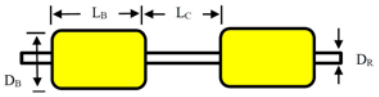

Fig.2 Definitions of L_C, L_B, D_R and D_B[1]

As illustrated in Table 1, three typical testing configurations C1, C4 , and C5 are chosen as the analyzing cases for present study. As shown in Figure 3, C1 and C5 refer to the configuration with 33% and 50% buoyancy modules coverage respectively, and C4 refers to the riser with 17% buoyancy modules coverage and half of the riser to the bottom end is covered with strakes. The detail dimensions and physical parameters are listed in Table 2 and 3 respectively.

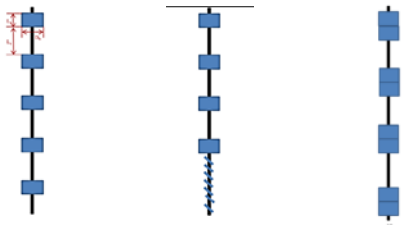

（a）C1　　（b）C4　　(c) C5

Figure 3 Riser configuration diagram for C1, C4 and C5[1]

Table 1 Selected cases for analysis

Test No.	5411	5470	5511	5570	5120
Riser Conf.	C1	C1	C4	C4	C5
Vel. (m/s)	0.5	1.05	0.5	1.04	0.6

Table 2 Configuration parameters for C1 & C4[1]

Riser	Spacing Ratio (*L*c/*L*b)	Aspect Ratio (*L*b/*D*b)	Diameter Ratio (*D*b/*D*r)	Coverage (%)
C1	2/1	1/1	5/1	33
C4	2/1	1/1	5/1	17
C5	1/1	2/1	5/1	50

Table 3 Physical properties of riser models[1]

Parameter	Units	Value
Total length between pinned ends	m	38
Element length	m	0.03
Bending stiffness, EI	$N.m^2$	572.3
Young modulus for pipe, E	N/m^2	3.46E10
Bare Pipe		
Outer diameter	mm	30
Wall thickness of fiberglass pipe	mm	15
Mass in air	kg/m	1.088
Mass in water	kg/m	0.579
Damping ratio	%	0.3
Buoyancy Element		
Outer diameter	mm	150
Length of each Buoyancy element	m	0.15
Mass in air (water filled)[1)]	kg/m	18.23
Strakes		
Pitch over diameter ratio	-	17.5
Height over diameter ratio	-	0.25
Outer diameter[2)]	mm	38.48
Mass in air (strakes only)	kg/m	0.5

[1)] includes mass of bare pipe;

[2)] which is used in calculating hydrodynamic coefficients of strake segments.

4. FEASIBILIY VALIDATION

The feasibility of present inverse analysis method was firstly validated against numerical simulation results from the empirical software VIVANA[6]. Firstly, the VIV displacement responses in CF direction of the bare riser (the same as shown in Table 3 in a sheared current(0.5m/s at left end, and zero at the right end) were calculated by VIVANA with its default hydrodynamic coefficient database [6]. The calculated excitation and added mass coefficients by VIVANA along the pipe were exported as well for the further comparisons with present inverse analysis results. Then taking the exported vibration displacement information as the inputs, the identified hydrodynamic coefficients in CF direction were obtained from inverse analysis method, which were then compared with the corresponding ones exported from VIVANA, as illustrated by Figure 4 and 5. It should be noted that the length of the element used for both VIV prediction and the inverse analysis in this case is set as 0.1m, which will be dense enough for the reconstructions of the displacements, velocities and accelerations on the nodes.

As we can see from Fig. 4 that the identified excitation force coefficients and the exported ones from VIVANA generally have good agreements. It should be noted that the differences become larger in the damping region with small current velocity. This is due to the “zero” current velocity at these regions, where a limited value of numerator with an "extremely small value" of the denominator (zero velocity) will induce a large value of result (the identified excitation coefficient) due to the mathematical algorithm used in the inverse analysis.

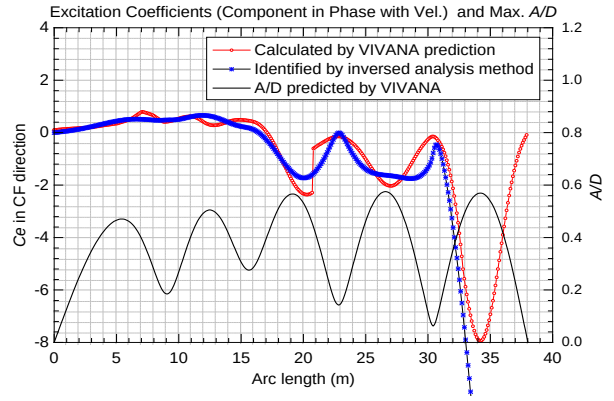

(a) Local comparison

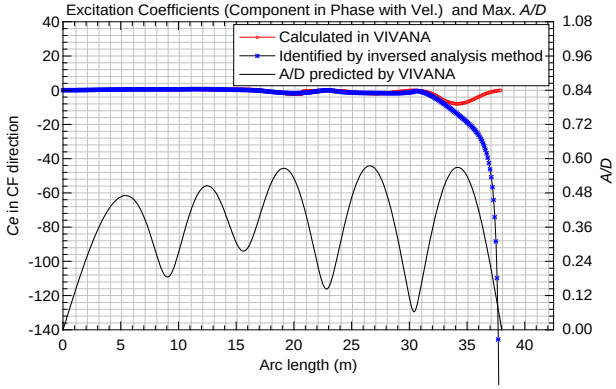

(b) Overall Comparison

Fig.4 Identified CF excitation force coefficients

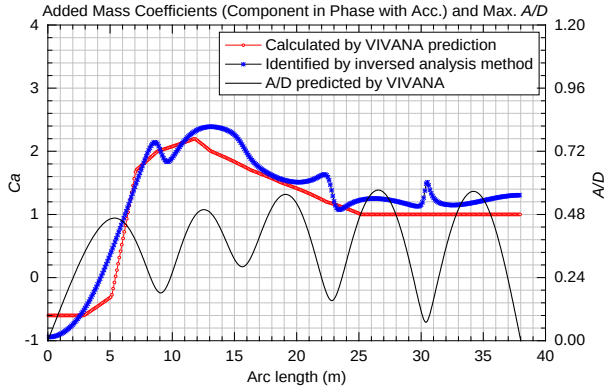

Figure 5 Identified CF added mass coefficients

As for the added mass coefficients in Fig.5, although some fluctuations are observed in the inversed results, the exported values and identified ones have generally pretty good agreement.

To further clarify the effects of these differences of coefficients shown in Fig.4-5, the vibration amplitudes calculated by the identified coefficients (directly by Eq.1) and those of inputs (predicted by VIVANA) were further compared, as illustrated by Fig.6. As we can see, the two dynamic displacements agree very well, which indicated that even with slightly different coefficients as inputs, the direct

calculating method and VIVANA could give the almost the same dynamic responses.

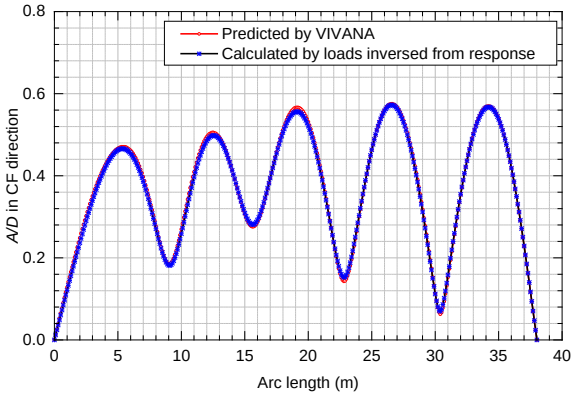

Figure 6. Vibration amplitudes calculated by Eq.1 from the identified coefficients and those by VIVANA

5. RESULTS AND DISCUSSIONS

The hydrodynamic coefficient distributions of the riser configurations C1 and C4 under current speed of 0.5 m/s and 1.05 m/s, C5 under 0.6m/s were taken as the examples to be discussed in this section.

It should be noted that from the FFT results of the measured vibration curvatures, several vibrating frequencies could be observed in each of the testing cases, which are corresponded with the base Strouhal frequencies of both bare and buoyancy segments, and higher order frequencies, as shown by Fig. 7. However, among the selected cases listed in Table 1, the dominating frequencies on C1 and C4 were corresponded with those of the Strouhal frequencies of the bare segment, and were particularly picked out for present analysis. And for configuration of C5, the dominating and picked frequency was corresponded with the Strouhal frequency of the buoyancy module.

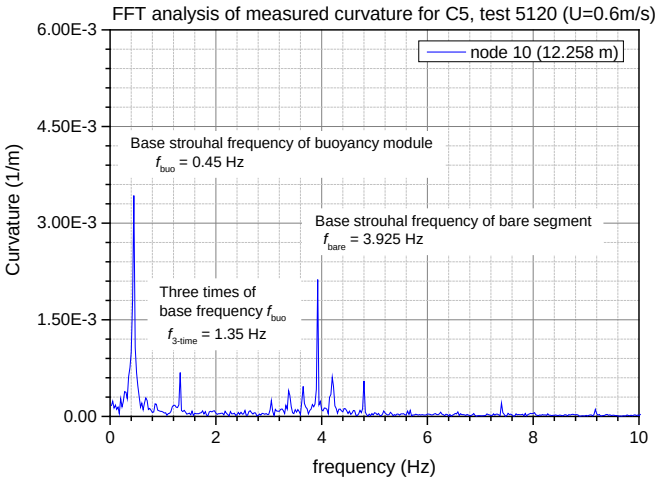

Fig.7 Typical FFT of a measured curvature signals in CF

5.1 Added Mass Coefficients

Figure 8 present the distribution of the added mass coefficients along the riser in CF direction for configuration C5 under towing velocity of 0.6 m/s.

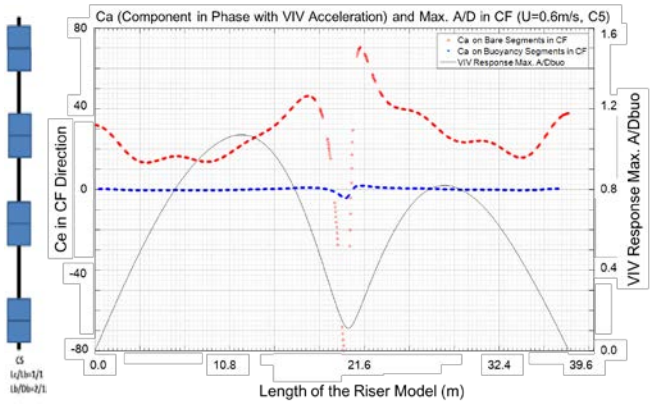

Figure 8 Identified CF added mass coefficients from a staggered buoyancy case C5 U=0.6m/s. The coefficients are corresponding to the buoyancy response frequency

Fig.8 shows that, out of the vibrating node area (around the mid-span of the riser), the added mass coefficients at bare segments are varying between 12 and 50, and between -0.20 and 0.2 on buoyancy elements; while around the vibrating node area, the added mass coefficients are varying between -80 and 70 on bare segments, and -4.0 and 2.0 on buoyancy elements. The large peak values around -80 and 70, are partly because of the small vibration amplitude around the node, which can be sensitive to error when decomposing forces into coefficients. The values of -4.0 to 2.0 are in the range of the contours from forced oscillation testing of a rigid cylinder. Regarding the surprising values of 12-50 on the bare segments, it could be explained as following:

Under the response frequency of the buoyancy, with length ration of *Lc*/*L*b=1/1, the water between the two adjacent buoyancy modules (around the bare pipe) will be trapped by these two buoyancy modules (with 15cm diameter), and forced to move together with the buoyancy modules. This makes the small bare pipe (with 3cm diameter) be bounded together with the trapped water, and oscillate like a virtual large buoyancy module (with a diameter of 5 times of the bare pipe). Based on this assumption, if the *Ca* of this "virtual buoyancy module" is of 1.0-1.2 (with respect to the volume of the buoyancy module), then by simple calculation we can find that the added mass coefficient with respect to the volume of the bare pipe will be in the range of 50-60, which is quite similar with present results.

Moreover, the eigen-frequencies with identified added mass coefficients were calculated, and compared with those of the measured response frequency. It shows that the second order

eigen-frequency is shifted from 0.56 Hz (on the dry structure) to 0.4 Hz (with identified added mass), which coincides with the measured response frequency of 0.4 Hz of the 2nd mode.

Figure 9 and Figure 10 present the distribution of added mass coefficients along riser in CF direction for C1 under U=0.5 m/s (test 5411) and U=1.05 m/s (test 5470) respectively. It shows that the added mass coefficients at bare segments are varying between 10 and 16, while are always in negative values on the buoyancy elements varying between -0.60 and -0.30. This similarity of added mass for two cases is due to that both cases are under the dominating frequency of the bare segment. Compared with those in Fig.8, the variation of the added mass values on the bare segments could be explained as following:

As foregoing analysis, under vibration conditions, the water between the two adjacent buoyancy modules (around the bare pipe) will be trapped by these two buoyancy modules (with 15cm diameter), and forced to oscillate together with the bare segment. If 100% water between the two adjacent buoyancy elements are assumed to trapped between two buoyancy modules when Lc/Lb=1 as shown in Fig.8, then when the spacing ratio Lc/Lb comes to 2/1 (C1 in present study), it will be straightforward and reasonable to assume that 50% water between the two adjacent buoyancy elements is trapped. This means that a Ca of 11 on the bare pipe, which is in the range of 10-16.

Additionally, it has found that the sum of the added mass and structural mass on the buoyancy modules should always be consistent with that of bare segments along the riser [12], as illustrated in Eq. (9).

$$(m_s + m_a)_{\text{bare}} = (m_s + m_a)_{\text{buo}} \tag{9}$$

where m_s is structural mass per unit length and m_a is added mass per unit length; the subscript 'bare' and 'buo' correspond to mass on bare segment and buoyancy module respectively. Thus, when the range of added mass coefficients on bare segment is 10 to 16, the added mass coefficient of buoyancy module can be simply calculated by,

$$C_{a,buo} = \frac{m_{a,buo}}{\frac{1}{4}\pi D_{buo}{}^2 \rho} = \frac{(m_s + m_a)_{bare} - m_{s,buo}}{\frac{1}{4}\pi D_{buo}{}^2 \rho} \tag{10}$$
$$= -0.33 \sim -0.57$$

which is quite similar with present results.

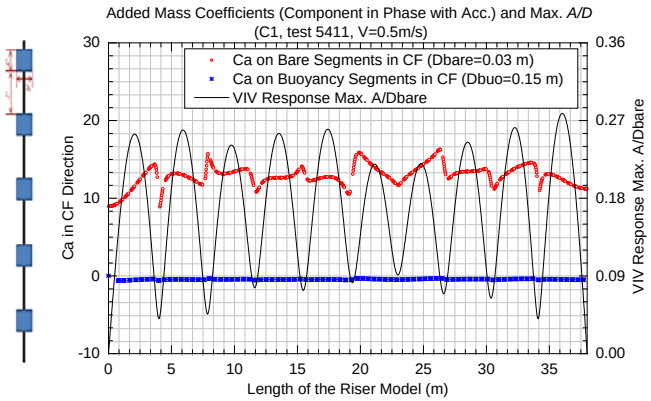

Figure 9 Identified CF added mass coefficients from a staggered buoyancy case C1 test 5411 (U=0.5 m/s). The force coefficients are corresponding to the bare response frequency 2.80 Hz. The filter pass band is 2.7 Hz to 2.9 Hz.

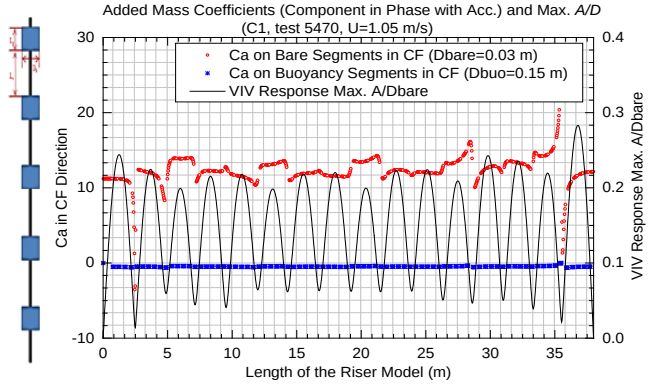

Figure 10 Identified CF added mass coefficients from a staggered buoyancy case C1 test 5470 (U=1.05 m/s). The force coefficients are corresponding to the bare response frequency 5.24 Hz. The filter pass band is 5.0 Hz to 5.5 Hz.

Figure 11 shows the distribution of added mass coefficients and non-dimensional amplitude A/D_{bare} along riser model in the CF direction for C4 under 0.5m/s current (test 5511).

The results show that the added mass coefficients for bare sections and buoyancy sections are in range of 8 to 20 and -0.6 to -0.3 respectively, which are quite similar with those of C1 (test 5411). The added mass coefficients on strakes sections are mostly in positive smaller values, except at the end where the added mass coefficients ramped from 0 to -4 within 1.5 meters. Besides, it clearly shows that the added mass coefficients of strakes nearby the bare parts (both buoyancy elements and pare pipe) are strongly affected by the neighboring buoyancy elements, and reached a value of 5.0. This kind of effects is also witnessed by the larger response amplitudes of the strakes parts nearby the buoyancy elements. This could be explained by the same reason as those for C1, where the added mass on the bare segment between two buoyancy modules was estimated

around 11. In current C4 condition, with only one buoyancy element left on the end side of the strakes, the trapped water will be reduced to ½ of those with two buoyancy elements (added mass of 11), and therefore the added mass on the adjacent strakes could be around 5.5, which is quite close to the current identified value of 5. Meanwhile, because of the fluidity of the water, the added mass should be linearly reduced from the buoyancy element regions with larger diameter to the pure strakes with smaller diameter, as shown by the variation of the added mass within the region of 19-20m of the pipe in Fig.10-11. While away from buoyancy region, the *Ca* on strakes segments varies within 1.0-3.5 with an average valued of 1.5.

The same trends can also be found for C4 under the current velocity of 1.04m/s, as illustrated by Figure 12.

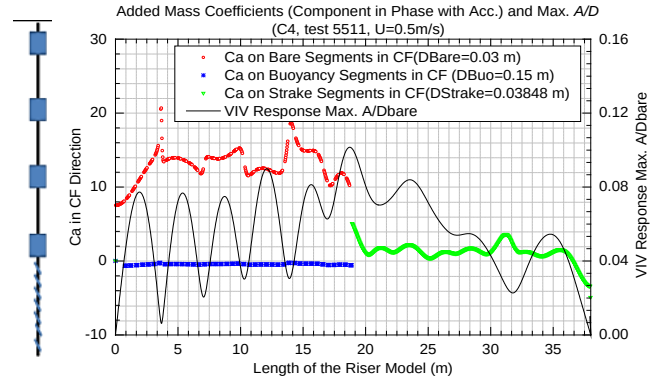

Figure 11 Identified CF added mass coefficients from a staggered buoyancy case C4 test 5511 (U=0.5 m/s). The force coefficients are corresponding to the bare response frequency 3.13 Hz. The filter pass band is 3.0 Hz to 3.3 Hz.

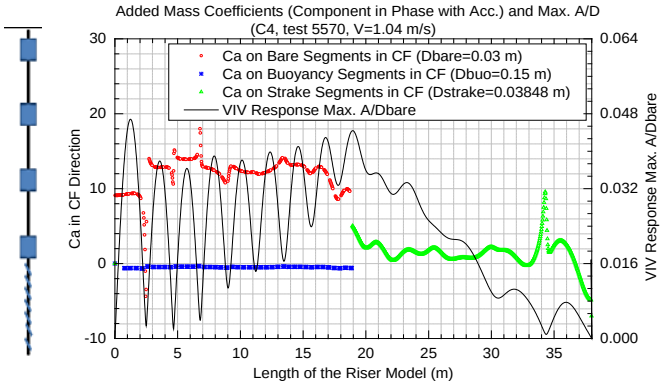

Figure 12 Identified CF added mass coefficients from a staggered buoyancy case C4 test 5570 (U=1.04 m/s). The force coefficients are corresponding to the bare response frequency 5.64 Hz. The filter pass band is 5.5 Hz to 5.8 Hz.

The eigen-frequencies calculated from the wet structure with identified mass and by the pure dry structure are listed in Table 4. As we can see, the identified added mass coefficients are again validated by the good agreements between the wet frequencies and the measured VIV response frequencies.

Table 4. Eigen-frequencies of the wet and dry structure

Test No.	5411	5470	5511	5570	5120
Riser Conf.	C1	C1	C4	C4	C5
Vel. (m/s)	0.5	1.05	0.5	1.04	0.6
Modal No.	10	16	9	14	2
Dry Fre.(Hz)	3.46	6.37	4.11	7.48	0.56
Wet Fre.(Hz) with identified added mass	2.81	5.27	3.16	5.83	0.4
Measured Response Fre.(Hz)	2.80	5.24	3.13	5.64	0.4

5.2 Excitation Coefficients

Figure 13 and Figure 14 presented the distribution of excitation coefficients along the riser in CF direction for C1 under U=0.5 m/s (test 5411) and U=1.05 m/s (test 5470) respectively. It can be seen that the magnitudes of excitation coefficients are varying from -0.7 to 0.55 on bare segments, and from -0.15 to 0.12 on buoyancy elements. And it's interesting that the ratio of the minimal/maximum ranges of the excitation coefficients between those on bare and on buoyancy segments is very close to the ratio of their hydrodynamic diameters 5.0 (D_{buo}/D_{bare}). Even though only the bare response frequency was picked for this hydrodynamic coefficients identification, the buoyancy segments are still always in the same excitation or damping regions as the adjacent bare sections, rather than always kept in the damping regions. This indicate that both bare and buoyancy segments are intent to "synchronous action" under one dominate frequency.

Moreover, the excitation coefficients shown in Fig.13-14, both on bare and buoyancy segments, are also showing the same "varying modes" as those on the displacement (10 in Fig.13 and 16 in Fig.10), which is different with the variation of the added mass coefficients.

Meanwhile, the excitation coefficients on both bare and buoyancy segments are intending to keep varying in a parabola shape between two vibration nodes with clear peak/bottom ranges. But it's not necessary for them to reach their peaks in phase with those of the displacements.

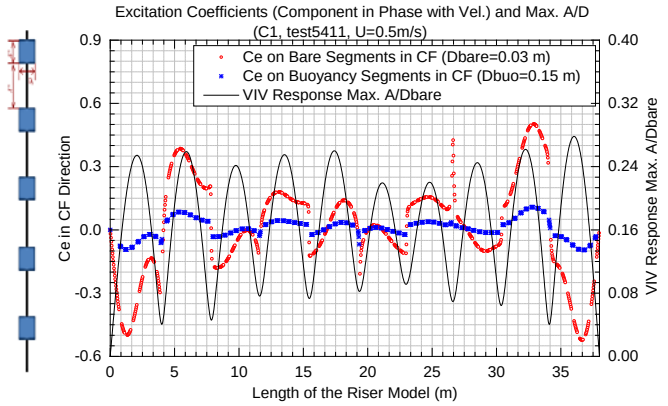

Figure 13 Identified CF excitation force coefficients from a staggered buoyancy case C1 test 5411 (U=0.5 m/s). The force coefficients are corresponding to the bare response frequency 2.80 Hz. The filter pass band is 2.7 Hz to 2.9 Hz.

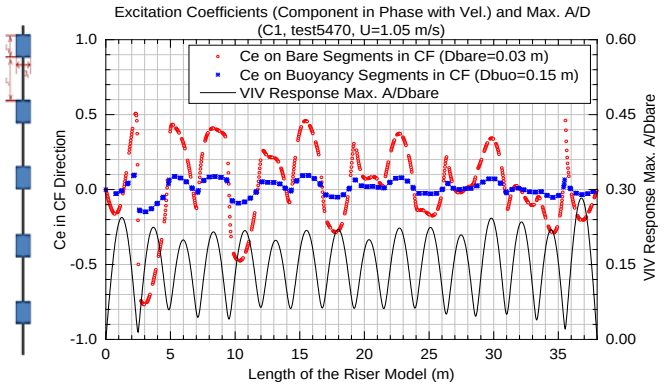

Figure 14 Identified CF excitation force coefficients from a staggered buoyancy case C1 test 5470 (U=1.05 m/s). The force coefficients are corresponding to the bare response frequency 5.24 Hz. The filter pass band is 5.0 Hz to 5.5 Hz.

Figure 15 illustrates the distribution of excitation coefficients along riser in the CF direction for C5 under U=0.6m/s. It can be seen that the magnitudes of excitation coefficients are varying from -0.7 to 1.7 for bare pipe, and from -0.15 to 0.5 for buoyancy elements. It should be noted that the excitation coefficients around the vibration node are in a relatively higher range on both bare and buoyancy segments. And different from those in Firg.13-14, the forces within one vibration node are not keeping to be always damping /excitation anymore, but are fluctuating between them.

Figure 16 shows the distribution of excitation coefficients and non-dimensional amplitude along the riser at CF direction for C4 case under 0.5m/s current (test No.5511). It can be found that the excitation coefficients on the bare and buoyancy segments have the same trends as foregoing presented: always in the same sign(positive or negative), and are mostly in excitation conditions; the magnitudes are in the range of -0.2 to 0.64 for the bare parts, and -0.04 to 0.13 for buoyancy part; the ratio of these two variation ranges is very close to the ratio of their outer diameters 5.0 (D_{buo}/D_{bare}). Meanwhile, as expected, the results clearly illustrated that the strakes covered parts of the riser are basically always damping the vibrations, where the excitation coefficients are around -0.1 and fluctuating between -0.5 and 0.06. It seems that there is ramp increasing of damping coefficients on the strakes nearby the bare and/or buoyancy elements. But it's very hard to establish the relationships between the damping coefficients and the vibration amplitude, frequency, reduced velocity or Re numbers.

The same trends can also be found for C4 under the current velocity of 1.04m/s, as illustrated by Figure 17.

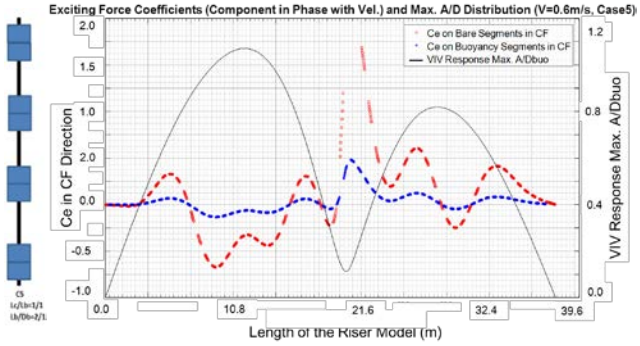

Figure 15 Identified CF excitation force coefficients from a staggered buoyancy case C5 U=0.6m/s. The force coefficients are corresponding to the buoyancy response frequency

The identified excitation coefficients on the strakes are further compared with those by Senga and Larsen [12], where thy conducted a series of forced motion experiments on a rigid cylinder with strakes of P17.5D/H0.25D, with non-dimensional displacement of 0.2 to 0.4. The observed range of excitation coefficients was reported within the range of 0 to -1, which is quite consistent with present identified values.

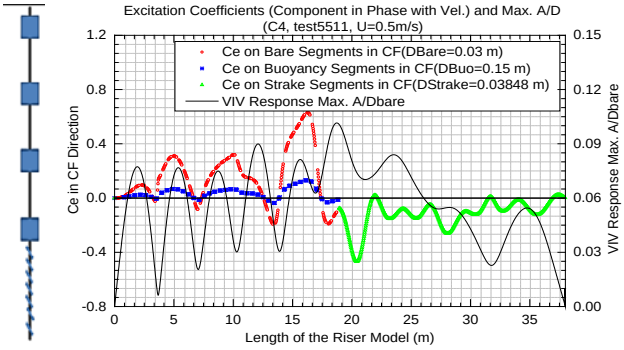

Figure 16 Identified CF excitation force coefficients from a staggered buoyancy case C4 test 5511 (U=0.5 m/s). The force coefficients are corresponding to the bare response frequency 3.13 Hz. The filter pass band is 3.0 Hz to 3.3 Hz.

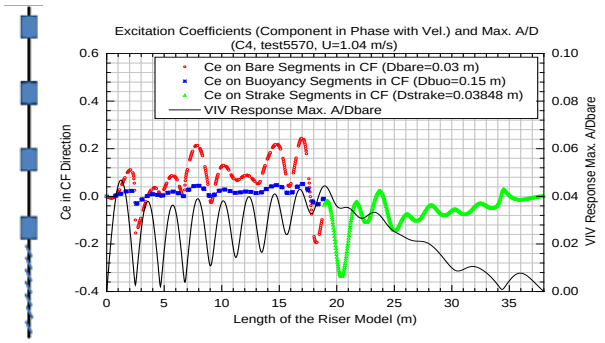

Figure 17 Identified CF excitation force coefficients from a staggered buoyancy case C4 test 5570 (U=1.04 m/s). The force coefficients are corresponding to the bare response frequency 5.64 Hz. The filter pass band is 5.5 Hz to 5.8 Hz.

5.3 Comparison of the Response Amplitudes

The dynamic responses of the riser have been reconstructed by:

1) Calculate the total hydrodynamic force (on the right side of Eq.1) from the identified coefficients.
2) Input the measured tension force from the experiments, and calculate the corresponding geometry stiffness on the left side of Eq.1.
3) With all of the dry structural information, and hydrodynamic forces, calculate the dynamic responses of the structure.

Finally the comparisons between these reconstructed responses and those of the measured are illustrated by Fig.18-19.

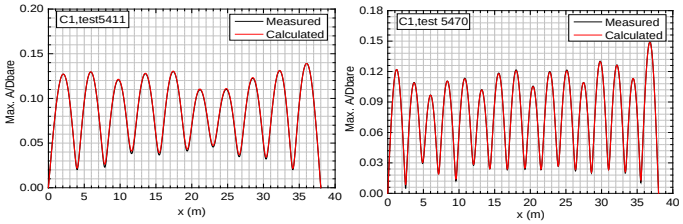

(a) U=0.5m/s (b) U=1.05m/s

Figure 18 Reconstructed and measured maximum A/D on riser model of configuration C1

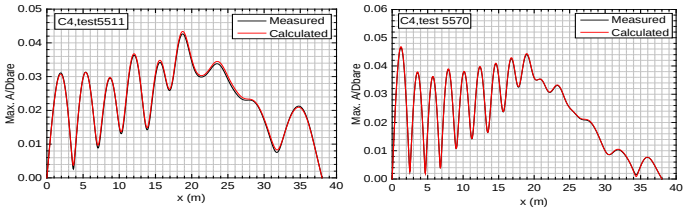

(a) U=0.5m/s (b) U=1.04m/s

Figure 19 Reconstructed and measured maximum A/D on riser model of configuration C4

As we can see from Fig.18-19, the results matched each other very well, which further illustrated the reliability of the numerical algorism used in this paper.

6. COMPARISON WITH FORCED OSCILATION TEST RESULTS

The identified coefficients are further compared with those by the forced oscillation tests of rigid cylinder[3] as illustrated by Figure 20-21.

Fig.20 presented the added mass coefficients identified from flexible model testing results and those from the forced oscillation tests[3].

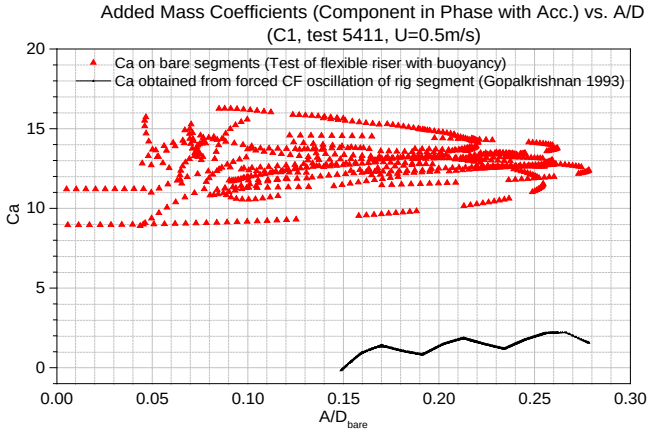

(a) *Ca* on the bare segments（C1, 5411, Vr=5.95）

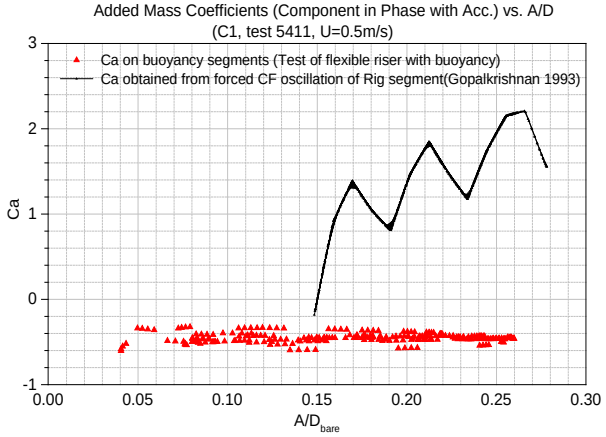

(b) *Ca* on the buoyancy elements（C1, 5411, Vr=5.95）

Fig. 20 Added mass coefficients from different ways

As we can see that the added mass coefficients on the bare segment between two buoyancy modules identified from flexible model testing are tremendous deviated from those by forced oscillation testing of a rigid bare pipe[3]. It should also be noted that even under the same vibrating frequency and amplitude, the added mass coefficients at different cross sections identified from the flexible model testing will vary a lot (as shown by the red triangular in the Figures), which is

due to the phase angle variation between the IL and CF vibrations at different stations along the pipe. The added mass on the buoyancy segments is always be negative identified from the flexible model testing, while in positive from the forces oscillation test.

Furthermore, the added mass coefficients of 10-15 identified are found close with those around 9 obtained from the corresponding forced oscillation tests on the corresponding rigid bare-buoyancy segment, where the same frequency and close amplitude was applied[14], while around -0.5 identified on the buoyancy elements and 1.9 from the forced oscillation tests.

Fig.21, presented the exciting force coefficients identified from flexible model testing and those from the forced oscillation tests of a rigid bare pipe [3].

The identified force coefficients are further divided into two groups: coefficients associated with displacement phase angle 0-180 degrees corresponded with counterclockwise orbits are marked by blue circles, and the ones with 180-360 degrees phase angles corresponded with clockwise are marked by red circles.

As we can see from Fig.21, the identified coefficients in phase between 0-180 degrees are mostly in positive values, and in similar range with those of the forced oscillation testing on a bared rigid cylinder. The similarities are because: since the diameter of the buoyancy elements are 5 times of the bare pipe, and could behave like "end plates" of the bare pipe, which therefore lead these similarities. The coefficients in phase between 180-360 degrees are mostly in negative, which is in anti-phases with those of the forced oscillation tests.

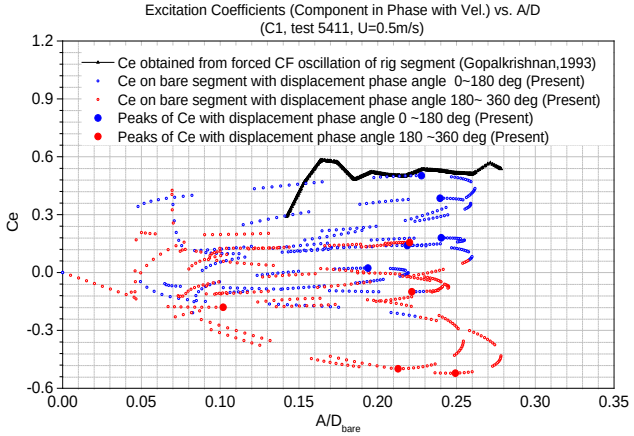

(a) *Ce* on the bare segments（C1, 5411, Vr=5.95）

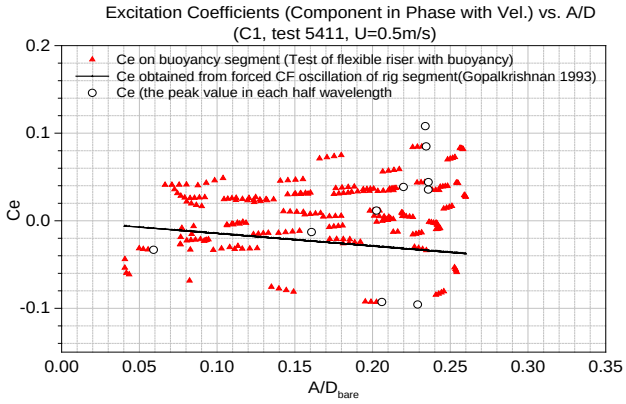

(b) *Ce* on the buoyancy elements（C1, 5411, Vr=5.95）

Fig. 21 Exciting force coefficients from different ways

Except the negative parts, the range of the positive exciting force coefficients of 0-0.3 identified on the bare segment are found quite relevant with those around 0.3 obtained from the forced oscillation tests on the corresponding rigid bare-buoyancy segments, where the same frequency and close amplitude was applied[14]. And the exciting force coefficient are around 0 identified on the buoyancy elements and -0.5 from the forced oscillation tests[14].

Compared with the bare segments, both the added mass and exciting force identified on the buoyancy segments are in a tremendous difference with those of the forced oscillation tests on a pure bared pipe [3]. This is though because the present identifications are from the bare segments vibrations dominating frequency, where the vibrations of the buoyancy elements was a kind of "forced motions" and kept in the same exciting/damping regions as bared segments, but couldn't get enough energy to reach their resonate conditions. The guess of the reason will be further confirmed by more comparisons between the identified coefficients from configuration C5 and those from the forced oscillation test on the corresponding rigid segments of C5[14].

7. CONCLUSIONS

In this paper, the inverse analysis method on a pipe with staggered buoyancy is presented. This method was firstly validated by the numerical tests through the comparisons with the known inputs/outputs parameters of VIVAN.

The inverse analysis method was then applied on the identification of the hydrodynamic coefficients from the experimental data of a flexible pipe with buoyancy elements and strakes under VIV conditions tested in SINTEF Ocean. Distributions of added mass and excitation coefficients along the model were investigated.

The results indicate that, the water around the bare segments between the two adjacent buoyancy segments will be

trapped and forced to oscillate together with the bare segments, and therefore will make the corresponding added mass coefficients even reach value of 50. This added mass coefficient should vary with the ratio of the length between bare and the adjacent buoyancy elements, e.g. 50 with 1:1 and 20 under 2:1, which are comparable with those from the corresponding forced oscillation tests. While the added mass on the buoyancy modules will fluctuate around zero, and almost always be in negative e.g. -0.6 to -0.3, under the vibration frequencies of the bare segments, and be within -2 to 6 under buoyancy elements vibrating frequency.

On the contrary, the excitation coefficients on the bare segments are within the same range as those from the CF forced oscillation tests of both rigid bare cylinder and rigid bare-buoyance cylinder, but are different with those on the buoyancy elements in terms of the amplitudes. It seems that the excitation coefficients by forced oscillation tests are most likely corresponded with those of the flexible model tests results with CF and IL vibrating phase angle of 0-180 degrees. The excitation coefficients on both bare segments and buoyancy elements are always kept in the same intensions in terms of excitation or damping the vibration. And the ratio of these two coefficients is close to the ratio of their outer diameters 5.0 (D_{buo}/D_{bare}).

Besides, the excitation coefficients on the strakes almost always keep in negative as expected, and are in the same ranges as those from forced oscillation tests [13], and more fluctuations and larger amplitude are observed.

The reliability of these identified hydrodynamic coefficients have been validated by the forced oscillation testing results, and comparisons of wet frequencies with measured response frequencies, and reconstructed vibration responses with those of tests.

REFERENCES

[1] Wu J., 2015, NDP Staggered Buoyancy VIV Test Report, Marintek Report, MT2015 F-098.

[2] Song L., Fu S., Cao J., Ma L., Wu J. 2016A. An investigation into the hydrodynamics of a flexible riser undergoing vortex-induced vibration. Journal of Fluids and Structures, 63, 325–350.

[3] Gopalkrishnan R. 1993. Vortex-induced Forces on Oscillating Bluff Cylinders. PhD thesis. Department of Ocean Engineering, Massachusetts Institute of Technology, Cambridge, MA, USA.

[4] Aronsen, K.H. 2007. An Experimental Investigation of In-line and Combined In-line and Cross-flow Vortex Induced Vibrations. PhD Thesis. Department of Marine Technology, NTNU, Trondheim, Norway.

[5] Vandiver J.K., SHEAR7 User Guide 4.5. 2003. Department of Ocean Engineering, Massachusetts Institute of Technology, Cambridge, MA, USA.

[6] Larsen C.M., Yttervik R., Passano E., Vikestad K. 2001. VIVANA Theory Manual. Version 3.1. Trondheim, Norway.

[7] Dahl, M. J. 2008. Vortex-Induced Vibration of a Circular Cylinder with Combined In-line and Cross-Flow Motion. PhD thesis, Department of Ocean Engineering, Massachusetts Institute of Technology, Cambridge, MA, USA.

[8] Soni, P.K. 2008. Hydrodynamic Coefficients for Vortex-induced Vibrations of Flexible Beams. PhD Thesis. Department of Marine Technology, NTNU, Trondheim, Norway.

[9] Yin D., Larsen C.M. 2011. Experimental and Numerical Analysis of Forced Motion of a Circular Cylinder. Proceedings of Offshore Mechanics and Arctic Engineering Conference 2011, OMAE2011-49438,June 2011, Rotterdam, The Netherlands.

[10] Wu J., Lie H., Larsen CM., Liapis S, Baarholm R. 2016. Vortex-induced vibration of a flexible cylinder: Interaction of the in-line and cross-flow responses. Journal of Fluids and Structures, 63 (2016) 238–258.

[11] Song L., Fu S., Zeng Y., Chen Y.. 2016B. Hydrodynamic Forces and Coefficients on Flexible Risers Undergoing Vortex-Induced Vibrations in Uniform Flow. J. Waterway, Port, Coastal, Ocean Eng., Volume 142, Issue 4.

[12] Zhang M., Fu S., Song L., Wu J., Lie H., Ren H. 2017. Hydrodynamics of flexible pipe with staggered buoyancy elements undergoing vortex-induced vibrations, OMAE 2017-61265.

[13] Senga H., Larsen C. M. 2017. Forced motion experiments using cylinders with helical strakes. Journal of Fluids & Structures, 68, 279-294.

[14] Wu J., Lie H., Fu S., Baarholm R. Constantinides Y. 2017, VIV responses of riser with staggered buoyancy elements: forced motion test and numerical prediction, OMAE 2017-61768.